COMMERCE
PUBLICATION

NOAA Technical Report ERL 283-WPL 26

U.S. DEPARTMENT OF COMMERCE
NATIONAL OCEANIC AND ATMOSPHERIC ADMINISTRATION
Environmental Research Laboratories

FM/CW Radar Signals and Digital Processing

DONALD E. BARRICK

BOULDER, COLO.
JULY 1973

ENVIRONMENTAL RESEARCH LABORATORIES

The mission of the Environmental Research Laboratories is to study the oceans, inland waters, the lower and upper atmosphere, the space environment, and the earth, in search of the understanding needed to provide more useful services in improving man's prospects for survival as influenced by the physical environment. Laboratories contributing to these studies are:

Earth Sciences Laboratories (ESL): Seismology, geomagnetism, geodesy, and related earth sciences; earthquake processes, internal structure and shape of the earth and distribution of the earth's mass.

Atlantic Oceanographic and Meteorological Laboratories (AOML): Geology and geophysics of ocean basins, oceanic processes, and sea-air interactions (Miami, Florida).

Pacific Oceanographic Laboratories (POL): Oceanography with emphasis on the oceanic processes and dynamics; tsunami generation, propagation, modification, detection, and monitoring (Seattle, Washington).

Atmospheric Physics and Chemistry Laboratory (APCL): Processes of cloud and precipitation physics; chemical composition and nucleating substances in the lower atmosphere; and laboratory and field experiments toward developing feasible methods of weather modification.

Air Resources Laboratories (ARL): Diffusion, transport, and dissipation of atmospheric contaminants; development of methods for prediction and control of atmospheric pollution; geophysical monitoring for climatic change (Silver Spring, Maryland).

Geophysical Fluid Dynamics Laboratory (GFDL): Dynamics and physics of geophysical fluid systems; development of a theoretical basis, through mathematical modeling and computer simulation, for the behavior and properties of the atmosphere and the oceans (Princeton, New Jersey).

National Severe Storms Laboratory (NSSL): Tornadoes, squall lines, thunderstorms, and other severe local convective phenomena directed toward improved methods of prediction and detection (Norman, Oklahoma).

Space Environment Laboratory (SEL): Solar-terrestrial physics, service and technique development in the areas of environmental monitoring and forecasting.

Aeronomy Laboratory (AL): Theoretical, laboratory, rocket, and satellite studies of the physical and chemical processes controlling the ionosphere and exosphere of the earth and other planets, and of the dynamics of their interactions with high altitude meteorology.

Wave Propagation Laboratory (WPL): Development of new methods for remote sensing of the geophysical environment with special emphasis on optical, microwave and acoustic sensing systems.

Weather Modification Program Office (WMPO): Plans and directs ERL weather modification activities, operates ERL aircraft fleet, and research on cumulus cloud modification, on hurricanes and other tropical problems, and on hurricane modification.

NATIONAL OCEANIC AND ATMOSPHERIC ADMINISTRATION

BOULDER, COLORADO 80302

U.S. DEPARTMENT OF COMMERCE
Frederick B. Dent, Secretary

NATIONAL OCEANIC AND ATMOSPHERIC ADMINISTRATION
Robert M. White, Administrator
ENVIRONMENTAL RESEARCH LABORATORIES
Wilmot N. Hess, Director

NOAA TECHNICAL REPORT ERL 283-WPL 26

FM/CW Radar Signals and Digital Processing

DONALD E. BARRICK

This work was sponsored in part by the
Defense Advanced Research Projects Agency

BOULDER, COLO.
July 1973

For sale by the Superintendent of Documents, U. S. Government Printing Office, Washington, D. C. 20402

NOTICE

The NOAA Environmental Research Laboratories do not approve, recommend, or endorse any proprietary product or proprietary material mentioned in this publication. No reference shall be made to the NOAA Environmental Research Laboratories, or to this publication furnished by the NOAA Environmental Research Laboratories, in any advertising or sales promotion which would indicate or imply that the NOAA Environmental Research Laboratories approve, recommend, or endorse any proprietary product or proprietary material mentioned herein, or which has as its purpose an intent to cause directly or indirectly the advertised product to be used or purchased because of this NOAA Environmental Research Laboratories publication.

TABLE OF CONTENTS

		Page
ABSTRACT		v
1.	OBJECTIVE	1
2.	APPLICATION	1
3.	TRANSMITTED WAVEFORM	1
4.	RECEIVED WAVEFORM	2
5.	DECHIRPED SIGNAL	3
6.	DOUBLE-FFT DIGITAL PROCESSING	7
7.	SINGLE FFT DIGITAL PROCESSING	12
8.	NUMBER OF COMPUTER OPERATIONS REQUIRED	16
9.	WINDOWING AND WEIGHTING	18
10.	RULES FOR SIGNAL DESIGN	19
11.	SATISFACTION OF REQUIRED ASSUMPTIONS	20
12.	SUMMARY	21
13.	REFERENCES	22

ABSTRACT

The use and processing of the FM/CW signal for radar and acoustic sounder systems are examined in this note. This signal--along with real-time digital processing via minicomputers--is currently being used by several groups for HF over-the-horizon radars. A comparative analysis of the different processing techniques for general radar applications has yet to be undertaken. This note therefore attempts to promulgate details of these techniques so that they may find use in other systems. An example involving an HF backscatter radar is used to permit the reader to see how the techniques are applied to an actual problem.

A linearly swept-frequency signal format is used in a 100% duty-factor mode. In the receiver, a replica of the linear FM signal is mixed with the received waveform at an offset such that the desired range window is observed with the lowest possible IF frequency variation. This pulse train is then analog-to-digital (A/D) converted and ready for computer processing. Two techniques are described and analyzed for digitally processing the signal via the Fast-Fourier-Transform (FFT) algorithm. The first is a double-FFT process; the first FFT set is done within a pulse-repetition-interval (PRI) to give range information. The next FFT set is done over N PRIs to give Doppler information. In the second technique, a single long FFT is used over N PRIs, giving simultaneously both range and Doppler information. It is shown that both techniques are identical, in that they produce the same information and require the same number of computer steps in executing the required FFTs. Both techniques yield *unambiguous* range and Doppler, for both discrete and distributed targets; the note shows how and where this information is contained in the processor output. The note also describes how two weighting functions are normally applied to the pulse train time samples to reduce objectionable range and Doppler sidelobes. Finally, simple "cookbook" rules are given for obtaining the signal and processing parameters based on the radar and target range/velocity specifications.

FM/CW RADAR SIGNALS AND DIGITAL PROCESSING

Donald E. Barrick

1. OBJECTIVE

The objective of this note is to present a simple and concise analysis--backed by an example--of the application of an FM/CW signal format in radar systems. It is shown how both time-delay (range) and Doppler (radial velocity) information can be extracted unambiguously.

2. APPLICATION

For the sake of illustration throughout these notes, we pick the following application and example. The HF radar carrier frequency is to be 10 MHz. Sea scatter is to be observed from the radar out to a range of 150 km (corresponding to time delays up to 1 millisecond in a back-scatter radar). It is known that HF sea scatter is confined spectrally to frequencies within about 1/3 Hz of the carrier. Therefore a pulse-repetition-frequency, f_r, of 1 per second is selected so that all echo Dopplers within $\pm$ 0.5 Hz of the carrier will be displayed unambiguously. To show sufficient detail, a Doppler processing resolution better than 0.02 Hz is desired, and a range resolution of the order of 1.5 km is desired; the latter two requirements in an ordinary pulse-Doppler system translate to a coherent integration time exceeding 50 seconds and a signal bandwidth of 100 kHz, respectively,

3. TRANSMITTED WAVEFORM

We select a 100% duty factor signal whose frequency sweeps upward, linearly, over one pulse-repetition-interval T_r ($T_r = 1/f_r = 1$ sec for our example). Since a 100 kHz signal bandwidth is desired, the signal can be written

$$v_T(t) = \cos[\omega_c t + \pi B f_r t^2] \equiv \cos[\phi_T(t)] \tag{1}$$

for $-T_r/2 < t < T_r/2$. It is assumed that the signal is periodic, and hence phase-coherent from one repetition interval to the next.

Since the instantaneous frequency, $f_T(t)$, is the derivative of the phase, we have

$$f_T(t) = \frac{1}{2\pi} \frac{d\phi_T(t)}{dt} = f_c + Bf_r t, \tag{2}$$

where here $f_c = 10$ MHz, $f_r = 1$ Hz, and $B = 100$ kHz. Thus it can be seen that the frequency excursion of $f_T(t)$ over one pulse-repetition interval is

$$\Delta f_T(t) = B = 100 \text{ kHz}. \tag{3}$$

The amplitude of the transmitted signal is taken to be unity. The plot of signal frequency vs time is shown in figure 1.

4. RECEIVED WAVEFORM

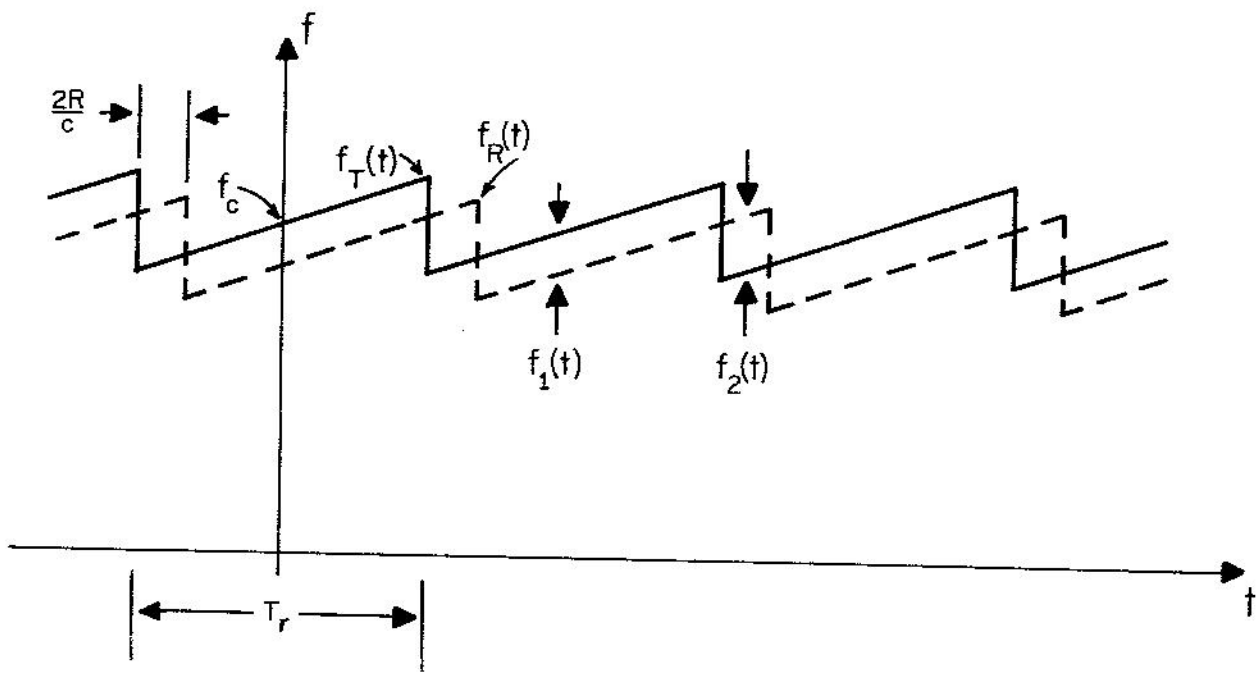

Figure 1. Frequency vs time of transmitted and delayed/Doppler shifted received signals.

The received signal is both delayed in time and shifted in Doppler. To illustrate the situation, we assume that we have a discrete target at range 15 km and travelling radially away from the radar at $v=5$ m/s (e.g., an ocean wave). At time $t=0$, the target is exactly at $R_0=15$ km from the radar. After that, its range is a function of time as

$$R(t) = R_0+vt \ . \tag{4}$$

The received signal from this discrete target is thus just a replica of the transmitted signal, but multiplied in amplitude by a factor A and delayed in position by a factor t_d, where $t_d = 2R(t)/c$. It is thus

$$v_R(t) = Av_T(t-t_d) = A\cos[\omega_c(t-t_d)+\pi Bf_r(t-t_d)^2] \ ; \tag{5}$$

its frequency is shown in figure 1 as the dashed curve.

5. DECHIRPED SIGNAL

Now after RF amplification, we mix the received signal with a replica of the transmitted signal; this is represented mathematically by subtracting a phase $\phi_T(t)$ from $\phi_T(t-t_d)$ to give a signal

$$v_1(t) = AP_T(t)\cos[\omega_c(t-t_d) - \omega_c t+\pi Bf_r(t-t_d)^2 - \pi Bf_r t^2] \ . \tag{6}$$

There is also a sum signal with phase $\phi_T(t)+\phi_T(t-t_d)$, but it is near $2\omega_c$ (twice the carrier), and hence removed by filtering. The function $P_T(t)$ denotes a pulse of unity amplitude and width T, where here, $T = T_r-t_d$.

Thus the mixture of the two sawtooth frequency waveforms and their subtraction, as shown in figure 1, produces a signal whose frequency format, $f_I(t)$, is as shown in figure 2. The two frequencies are

$$f_1 = \frac{1}{2\pi}\frac{d}{dt}[\phi_T(t-t_d) - \phi_T(t)] \ , \tag{7a}$$

and

$$f_2 = \frac{1}{2\pi}\frac{d}{dt}\left[\phi_T(t-t_d) - \phi_T(t+T_r)\right] \quad . \tag{7b}$$

The intermediate, dechirped signal can be represented as the sum of two pulse trains as shown in figure 2. One, $v_1(t)$, is at frequency f_1, and the width of these pulses is $T = T_r - t_d$. The other, $v_2(t)$, is at frequency f_2, and the width of the pulses is $T = t_d$. It will be possible to eliminate $v_2(t)$ by filtering if $f_2 \gg f_1$; such will be the case here.

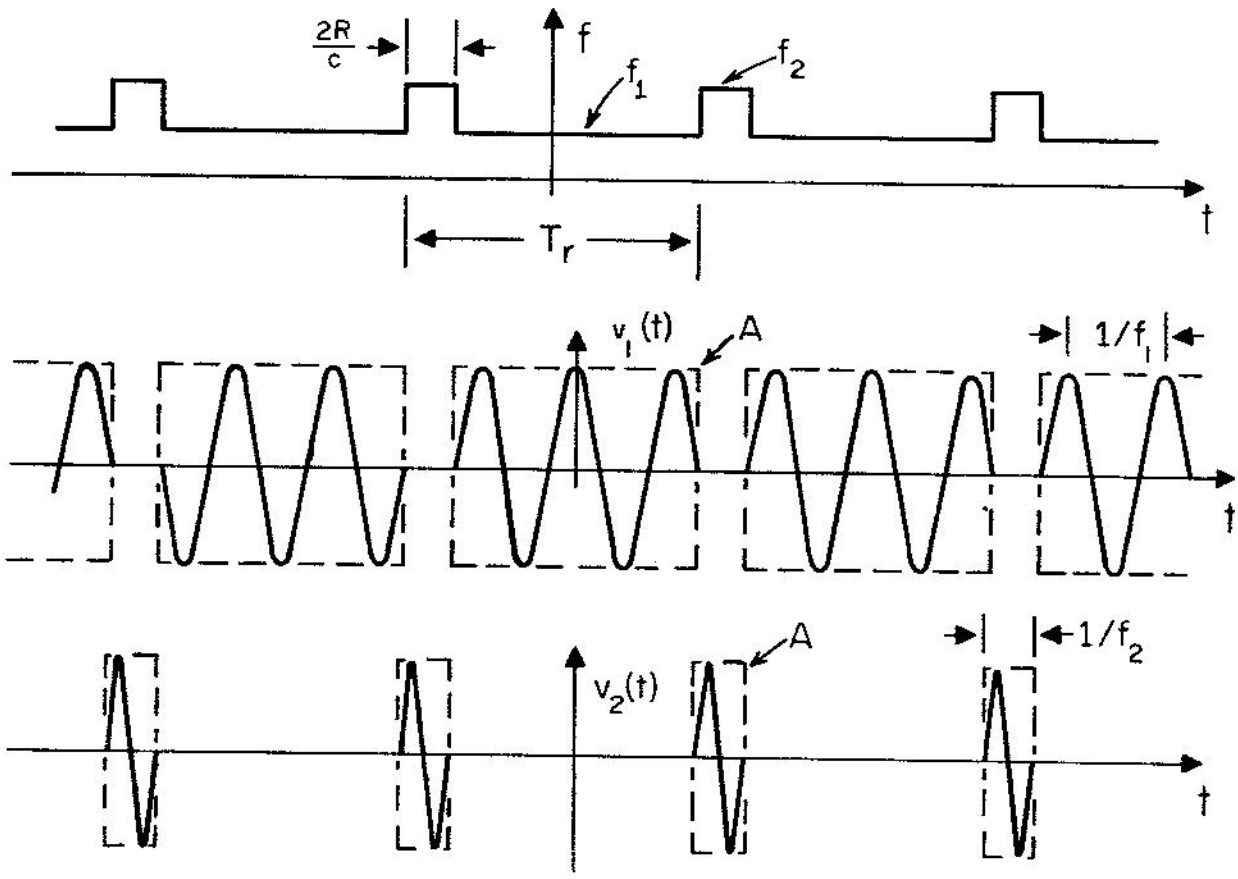

Figure 2. Frequency and amplitude plots vs time of received signal after dechirping.

Therefore, we are left with a single pulse train to analyze, as represented by equation (6). It is possible to re-center the time origin so that it falls in the middle of the first pulse; this is done in figure 2. The frequency and phase from pulse to pulse are changing very slightly, however; we will analyze this now.

5.1 $-T_r/2 < t < T_r/2$

Let us simplify the phase in the first pulse; denote internal time, t, within this pulse as t_i. Using $t=t_i$ and $t_d=2R/c=2R_0/c+2vt/c\equiv t_0+2vt_i/c$, (where $t_0\equiv 2R_0/c$ is the initial delay of the signal), we have $\phi_I(t_i)\equiv\phi_T(t_i-td)-\phi_T(t_i)$, or

$$\phi_I(t_i) = [-2\pi f_c t_0+\pi B f_r t_0^2] + 2\pi[-2\,\frac{v}{c}\,f_c+Bf_r t_0\,\frac{2v}{c}-Bf_r t_0]t_i$$

$$-2\pi B f_r\cdot\frac{2v}{c}\,(1-\frac{v}{c})t_i^2 \quad . \tag{8}$$

Thus we have three contributions to the phase: a constant, a linear term in time t_i, and a quadratic term in time, t_i^2. For the parameters of the example, however, the quadratic phase term is always small within the interval $-T_r/2 < t_i < T_r/2$; e.g., at $t_i=T_r/2$, it is of the order of 0.005 radian. Also, it can be shown that the second term in the linear factor is small compared to the first term and is also much less than one radian. Of course, in all cases under consideration here, $v/c \ll 1$, i.e., target velocity is small compared to propagation velocity. Therefore we have

$$\phi_I(t_i)\simeq\phi_0-2\pi[\,\frac{2v}{c}\,f_c+Bf_r t_0]t_i \quad ; \tag{9}$$

hence within the first pulse, the frequency f_I is

$$f_I = \frac{2v}{c}\,f_c+Bf_r t_0 \quad . \tag{10}$$

As can be seen, this frequency offset (also shown in the preceding figure) consists of two terms: the first due to the target velocity and the second due to the time delay (or range) to the target ($t_0=2R_0/c=0.1$

millisecond for R_0=15 km). For the example selected here, the second term (range term) is larger; i.e., $\frac{2v}{c} f_c = \frac{1}{3}$ Hz, $Bf_r t_0$=10 Hz. Thus it is not possible to separate range from target velocity by measuring frequency f_1 *within a single pulse.*

5.2 $(2n-1)T_r/2 < t < (2n+1)T_r/2$

Here we want to examine the phase in the n-th pulse, assuming that the n=0 pulse is the one centered at t=0. Again, we describe the time *within* the n-th pulse (from its own center) as t_i. The time delay to the target, t_d, however is now given by

$$t_d = 2R/c = 2R_0/c+2vt/c = t_0+2v(nT_r+t_i)/c \quad , \tag{11}$$

where we describe time to the center of the n-th pulse as nT_r. We can now substitute this into the phase:

$$\begin{aligned}\phi_{In}(t_i) &\equiv \phi_T(t_i-t_d) - \phi_T(t_i) \qquad (12)\\ &= -\omega_c t_0 - \omega_c \frac{2v}{c} t_i - \omega_c \frac{2v}{c} nT_r + \pi Bf_r[t_0+\frac{2v}{c}(nT_r+t_i)]^2 \\ &\qquad - 2\pi Bf_r[t_0+\frac{2v}{c}(nT_r+t_i)] \quad .\end{aligned}$$

After expansion and elimination of terms which are small compared to others and also small compared to one radian, we have (assume $n \leq 100$)

$$\phi_{In}(t_i) = \phi_0 - 2\pi f_c \cdot \frac{2v}{c} \cdot nT_r - 2\pi[\frac{2v}{c} f_c+Bf_r t_0 + \frac{2v}{c} Bn]t_i \quad ; \tag{13}$$

hence the frequency in the n-th pulse is the quantity in square brackets, i.e.,

$$f_{In} = \frac{2v}{c} f_c+Bf_r t_0+ \frac{2v}{c} Bn. \tag{14}$$

Comparison of (14) with (10) shows that the frequency in the n-th pulse is identical to that in the first pulse, with the exception of the

third term. The explanation for the third term is simple. It merely means that the target is moving from pulse to pulse, and its range at the center of the n-th pulse is $R_0+c(2v/c)nT_r/2 = R_0+vnT_r$, as we would expect. Since we want to integrate over as many as 100 pulses, the third term is not negligible as n increases; e.g., at $n=100$, $\frac{2v}{c} B_n = \frac{1}{3}$ Hz.

Two other effects occur within the pulse; its width, being $T=T_r-t_d$ changes very slightly from pulse to pulse. Since $T_r=1$ second, $t_d = t_0+(2v/c)nT_r$, we have for $n=1$, $T = 1-10^{-4}$ s; for $n=100$ we have $T = 1-10^{-4}-\frac{1}{3} \times 10^{-5}$ s. Thus the change in pulse width is negligible. A very important second effect, however, is the change in phase from pulse to pulse, as represented by the second term in (13). This phase change shall in fact prove to be the basis for the Doppler processing. As stated earlier, all of this assumes that the transmitted signal is phase-coherent, i.e., $\phi_T(t+T_r)-\phi_T(t)$ = non-varying constant.

6. DOUBLE-FFT DIGITAL PROCESSING

Here we want to demonstrate how a double Fourier-transformation process can be used--often in real time because of the discovery of the digital fast-Fourier-transform (FFT) algorithm--to produce a time-delay (range) and Doppler (velocity) display of the radar target data*. The first Fourier transform process is performed over a pulse repetition period, T_r (i.e., within a pulse) to obtain target range. The second Fourier transform is then performed over several pulses of these data to obtain target Doppler or velocity.

First, let us perform a Fourier transform on a single pulse. This is shown in figure 3. We have a pulse of width $T = T_r-t_d$, amplitude A, and frequency f_1 given by (14). To perform this Fourier transform digitally, one must sample the pulse M times within the time period T_r. The number M depends upon the maximum value f_1 can assume, and M/T_r must be at least twice this value, i.e., $2f_{1max}$, according to the Nyquist theorem. For the problem considered earlier where we want to

*This technique is currently being used by the Stanford Research Institute for real-time processing of HF ionospheric radar signals at their Wide Aperture Research Facility (WARF); (Sweeney, *et al.*, 1971).

display possible targets at all ranges from zero to 150 km, this corresponds to a frequency variation in f_1 from 0 to 100 Hz; hence M must be greater than 200 since T_r=1 sec. Since FFT processors require that $M=2^k$, where k is an integer, M=256 would suffice.

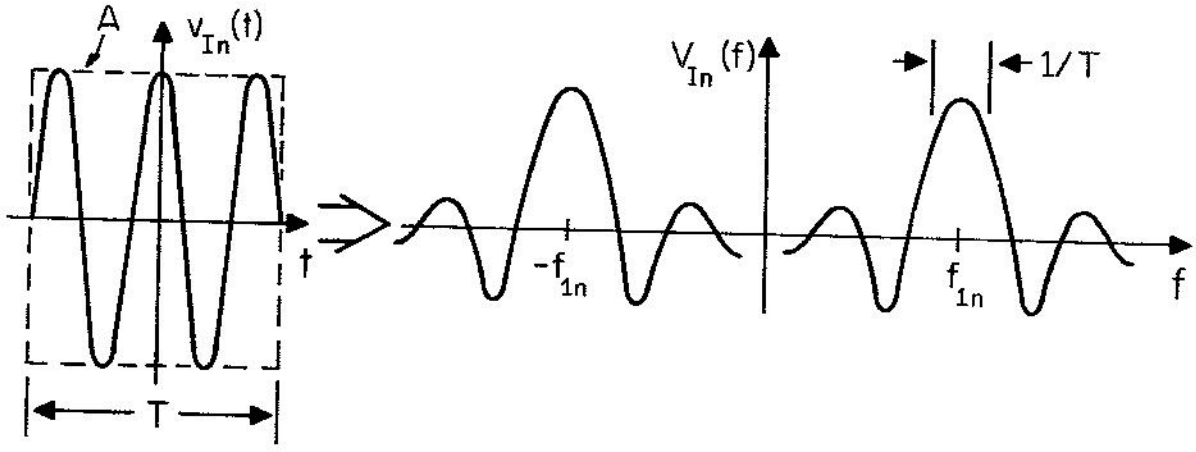

Figure 3. Single pulse and its Fourier transform.

The Fourier transform of the pulse is then

$$V_{In}(f) = \int_{-T/2}^{T/2} A[\cos\phi_{In}(t_i)]e^{-i2\pi f t_i}\, dt_i$$

or

$$V_{In}(f) = \frac{AT}{2}\left\{\frac{\sin[2\pi(f-f_{In})T/2]}{[2\pi(f-f_{In})T/2]}\, e^{-i\phi_0+i2\pi f_c\cdot\frac{2v}{c}nT_r} + \frac{\sin[2\pi(f+f_{In})T/2)]}{[2\pi(f+f_{In})T/2]}\, e^{+i\phi_0-i2\pi f_c\cdot\frac{2v}{c}nT_r}\right\} \quad . \qquad (15)$$

This Fourier transform is shown in figure 3. Since we started with $M=2f_{1max}T_r$ samples (M=200 minimum), we obtain samples in the frequency domain from $-f_{1max}$ to $+f_{1max}$, i.e., at $M/2=f_{1max}T_r$ positive values of frequency. These samples are complex in general, as evidenced by the exponential phase factor containing ϕ_0 and $2\pi f_c \frac{2v}{c} nT_r$. Thus we conceptually have M/2 range bins (M/2=100 here), permitting us to realize the 1.5 km range resolution over a 150 km window, as initially stipulated. Note that each M/2 resolution element after the first FFT can be considered a range bin so long as the Doppler term, $(2v/c)f_c$, is small compared to the range term, $Bf_r t_0$; this is true for the example considered here. Since each pulse is approximately 1/T wide at the half-power point ($T \simeq T_r = 1$ sec here), we should be able to resolve 100 targets in range because the width of each FFT pulse in this 100 Hz window is 1 Hz. Hence after one FFT process within a pulse we have range information, but no Doppler information; we turn now to extraction of Doppler.

Note that if we start with the first pulse at $n=1$ and do this FFT process on each pulse, we obtain a Fourier transform n times, where we assume $n \leq N$ (some upper value). Since the frequency, f_{1n}, and phase, $2\pi f_c \frac{2v}{c} nT_r$, shifts slightly from pulse to pulse due to target velocity (as given in (14)), this $\sin x/x$ pulse in the frequency domain will change very slightly after each Fourier transformation. Since our digital FFT is capable of producing numbers at M/2 discrete points, (15) should really be written with f replaced by $f = \frac{2m}{M} f_{1max}$, where $-M/2 \leq m \leq M/2$.

Thus the first FFT process on M samples within a pulse gives $M/2$ range bins for each pulse. For each successive pulse, this FFT gives $M/2$ additional positive frequency samples. Digitally, we store each $M/2$ samples in rows of a matrix, as shown in figure 4, until we have N rows. Thus, we have an $M/2$-by-N matrix whose columns so far represent range bins.

Now, we perform another FFT over each column, or range bin. This will require N points altogether. Each matrix element is a complex number whose value changes in a column because the frequency, f_{1n}, and the phase, $2\pi f_c \cdot \frac{2v}{c} nT_r$, are changing from sweep to sweep. Since each of the N vertical elements comes from a different pulse T_r sec apart,

NT_r sec are required to fill this matrix. Also, n can be related to time from the first pulse by use of $t=nT_r$, or $n=t/T_r$ (again, $1< n< N$). Hence each column is really a function of time, and the N column elements can be considered (digital) samples of this time function.

To Fourier transform over a typical column (say the m-th), let us again refer to our example for the target at R_0=15 km; this target will appear in the m=10 bin for M/2=100. As we saw before, this produces $f_{1n} = 10 + \frac{1}{3} + \frac{n}{3} \cdot 10^{-2}$ Hz. Thus for n running from 1 to 100--corresponding to time running between 1 and 100 seconds--two things happen to the positive pulse in the m-th range bin: its amplitude changes slightly due to the shift of the $\sin x/x$ pulse because of f_{1n}, and its phase changes. The amplitude variation from n=1 to n=100 is slow. For the example given, the shift in the pulse due to f_{1n} is $\frac{1}{3}$ Hz over N=100 pulses; the 3 dB width of the $\sin x/x$ pulse is 1/T=1 Hz while the total width between the first nulls is 2/T=2 Hz. Hence the amplitude variation within a column is slight, and can be represented in most cases by a constant or, for more accuracy, by a constant plus a small linearly varying term; the results will not differ significantly for either case. Hence we represent the amplitude by a constant (i.e., $\sin[2\pi(f-f_{1N/2})T/2]/[2\pi(f-f_{1N/2})T/2]$, its value midway down the column where n=N/2) and leave the second representation as an exercise to the interested reader.

$$\begin{array}{c} \longleftarrow \text{Range Bins} \longrightarrow \\ \begin{pmatrix} S_{11} & S_{12} \cdots & S_{1m} \cdots & S_{1M/2} \\ S_{12} & S_{22} \cdots & S_{2m} \cdots & S_{2M/2} \\ \vdots & & & \\ S_{n1} & S_{n2} \cdots & S_{nm} \cdots & S_{nM/2} \\ \vdots & & & \\ S_{N1} & S_{N2} \cdots & S_{Nm} \cdots & S_{NM/2} \end{pmatrix} \end{array}$$

Figure 4. Matrix containing range-Doppler numbers obtained with double-FFT process.

Thus the only variation now within the column (at the positive frequency corresponding to m) is the phase factor, i.e.,

$$S_{nm} = K(f)e^{i2\pi f_c \cdot \frac{2v}{c} nT_r} = K(f)e^{i2\pi f_c \frac{2v}{c} t_n} \text{ , where} \tag{16}$$

in the rightmost expression, nT_r has been replaced by t_n to represent the discrete flow of time from pulse to pulse. The Fourier transform of this quantity over t_n from 0 to NT_r is

$$\mathscr{S}_m = KNT_r \frac{\sin[2\pi(f-\frac{2v}{c}f_c)NT_r/2]}{[2\pi(f-\frac{2v}{c}f_c)NT_r/2]} \text{ , where} \tag{17}$$

here again we should note that our digital FFT does not really give a continuous variation over f (frequency), but will compute values at N discrete frequency points. The question arises as to how we should choose these N frequency points, i.e., how wide a frequency window do we want to display. Since our PRF, f_r(f_r=1 Hz here) results in an unambiguous Doppler of $\frac{1}{2}$ Hz, we would logically select $f_{Dmax} = \frac{1}{2} f_r$(= $\frac{1}{2}$ Hz here) so as to display all of the unambiguous Doppler window. Then the frequency window in Doppler will be from $-f_{Dmax}$ to $+f_{Dmax}$ at a spacing f_{Dmax}/N, which turns out to every $2f_{Dmax}/N$ Hz, or 1/100 Hz here. Note also in (16) that if $\frac{2v}{c} f_c$, i.e., the Doppler shift, exceeds $\frac{1}{2} f_r = 1/2T_r$, then from pulse to pulse we will be sampling at less than the required Nyquist sampling rate. Hence our pulse-repetition frequency (PRF), f_r, must always be *at least* twice as great as the maximum expected Doppler frequency.

Observe now an important fact in (17): the displacement of the $\sin x/x$ pulse resulting from the second Fourier transformation over the columns occurs at $\frac{2v}{c} f_c$. This is precisely the Doppler shift that results from a target at (radial) velocity v with a backscatter radar having carrier frequency f_c. Furthermore, the 3 dB width of the pulse represented by (17) is $1/NT_r$ Hz, as shown in figure 5. Thus we produce N (or 100) Doppler frequency points every f_r/N Hz (or .01 Hz here) having a Doppler resolution of $1/NT_r$ Hz (= .01 Hz here). Since NT_r is the coherent integration time (in this scheme, it is the time required to fill the matrix), $1/NT_r$ is exactly the Doppler resolution one would expect from any coherent pulse-Doppler radar.

Therefore, in summary, we have done two sets of FFTs. One set within each pulse at M points to give M/2 range bins; these bins are the elements of a row of a matrix. The second set is over N pulses, or over the N column elements of the matrix, to give N Doppler bins for each range bin. Note that the original target range also contained a small offset due to Doppler. If this offset is objectionable, it can now be removed--in the case of a discrete target--by using the Doppler information to correct the target range.

A little thought will show that this process also works for distributed targets such as rain or sea waves. If one has many targets in a range bin (say L targets), he has L terms in (15), and each element in the matrix is really the sum of L such terms. The second FFT over the columns, therefore by superposition, gives L terms in (17); if each of the L scatterers in the bin (representing the distributed target complex) has a different velocity, then the resulting Doppler spectrum for the L targets will consist of L-sinx/x pulses at different positions, as given by (17) and shown in figure 5. Thus a continuous Doppler spectrum represented by the sum of L scatterers with many different velocities and scattering amplitudes will result, as would be expected in any coherent pulse-Doppler radar system.

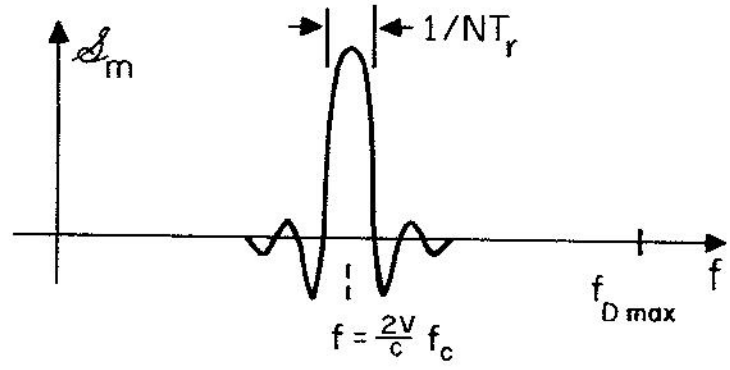

Figure 5. Doppler spectrum after second transformation within a given range bin.

7. SINGLE-FFT DIGITAL PROCESSING

Now we examine another technique for extracting range and Doppler information from the same signal. This involves a single, *long* FFT over

the same N pulses. This technique is used by the Rome Air Development Center for some of its HF over-the-horizon radars (Eddy, 1973). It involves the same number of computer operations as that described in the preceding section.

Here we will draw heavily on much of the material in the preceding section. Since we have a maximum frequency f_{1max} in our pulse $T_r(\approx T)$ seconds long, we require $M=2f_{1max}\cdot T_r$ samples per pulse, as before. Performing the FFT over N pulses gives a total of $M \times N$ samples per transform. Let us analytically find an expression for the Fourier transform of this pulse train first. To do this, we can use superposition to express the Fourier transform of the pulse train as the Fourier transform of each pulse as though it were all alone:

$$V_I(f) = \sum_{n=0}^{N-1} \int_{(2n-1)T_r/2}^{(2n+1)T_r/2} v_{In}(t)e^{-i2\pi ft}\, dt \quad . \tag{18}$$

Here we reexpress the phase $\phi_{In}(t_i)$ appearing in V_{In}--as given in (13)--in terms of continuous time, t, rather than time within a pulse, t_i. This is done by substituting $t_i=t-nT_t$ into (13) to give

$$\phi_{In}(t) = \phi_0 + 2\pi[Bt_0+ \frac{2v}{c} BnT_r]n-2\pi[\frac{2v}{c} f_c +Bf_rt_0+ \frac{2v}{c} Bn]t \ . \tag{19}$$

Using this in (18) and performing the indicated integration, we obtain (with the approximation $T_r\approx T$)

$$V_I(f) = \sum_{n=0}^{N-1} V_{In}(f)e^{-i2\pi fnT_r} \quad . \tag{20}$$

where $V_{In}(f)$ is given in (15) and discussed in that section.

Now, to perform the summation, we make the same assumptions as before; i.e., that of both the amplitude and phase variations over n which occur in $V_{In}(f)$, only the phase variation is important. Also we use only the first $\sin x/x$ function in (15) since it represents positive

frequencies; an identical result obtains for the second term representing the negative frequencies. Therefore, (20) becomes

$$V_I(f) = K(f)\sum_{n=0}^{N-1} e^{-i2\pi(f-\frac{2v}{c}f_c)nT_r} \tag{21}$$

where we have used (16). The above summation can be performed by using the identity:

$$\sum_{n=0}^{N} e^{in\alpha} = e^{iN\alpha/2} \cdot \frac{\sin[(N+1)\alpha/2]}{\sin[\alpha/2]} \quad . \tag{22}$$

Thus we obtain

$$V_I(f) = K(f)\,\frac{\sin[2\pi(f-\frac{2v}{c}f_c)NT_r/2]}{\sin[2\pi(f-\frac{2v}{c}f_c)T_r/2]}\, e^{-i2\pi(f-\frac{2v}{c}f_c)(N-1)T_r/2} \quad . \tag{23}$$

In the above final result, the complex exponential factor--as well as the residual phase factor $e^{i\phi_0}$ contained in $K(f)$--is not important because it has unity amplitude. However we note that the $\sin N\alpha/\sin\alpha$ is much like the $\sin N\alpha/N\alpha$ function. It contains a peak at $\alpha=0$ and side-lobes away from the peak; it is, however, periodic whereas $\sin N\alpha/N\alpha$ is not.

Now, we note that the FFT does not actually compute a continuous function, $F_I(f)$, but a transform at MN positive *and* negative frequency points. Since the maximum frequency, f_{1max}, is determined primarily by the maximum target range desired, we have MN/2 *positive* frequency points, and hence a value of $V_I(f)$ computed every $f = 2f_{1max}/(MN)$ Hz along the positive frequency axis.

To see how a discrete target will appear, we plot first in figure 6 the broad function representing the integration over a single pulse, i.e.,

$$K(f) = \frac{\sin[2\pi(f-f_{IN/2})T/2]}{[2\pi(f-f_{IN/2})T/2]} \quad . \tag{24}$$

This gives the range bin, or location of the target in range. Its center is slightly displaced, however, due to the Doppler term $\frac{2v}{c}f_c$ in $f_{IN/2}$.

Next we show the $\sin N\alpha/\sin\alpha$ factor of (23) in figure 6 for a moving target. Notice that it repeats itself at the pulse-repetition frequency, f_r, as one would expect in any pulse-Doppler radar. Note that this factor contains only Doppler information and would be identical for a target at any range having the same radial velocity.

Finally we show the product of the two functions for a moving target at a range corresponding to $f_{IN/2}$. Notice that the slowly varying range function essentially envelope modulates the Doppler function, now isolating the target in both range and Doppler. The range resolution is essentially the width

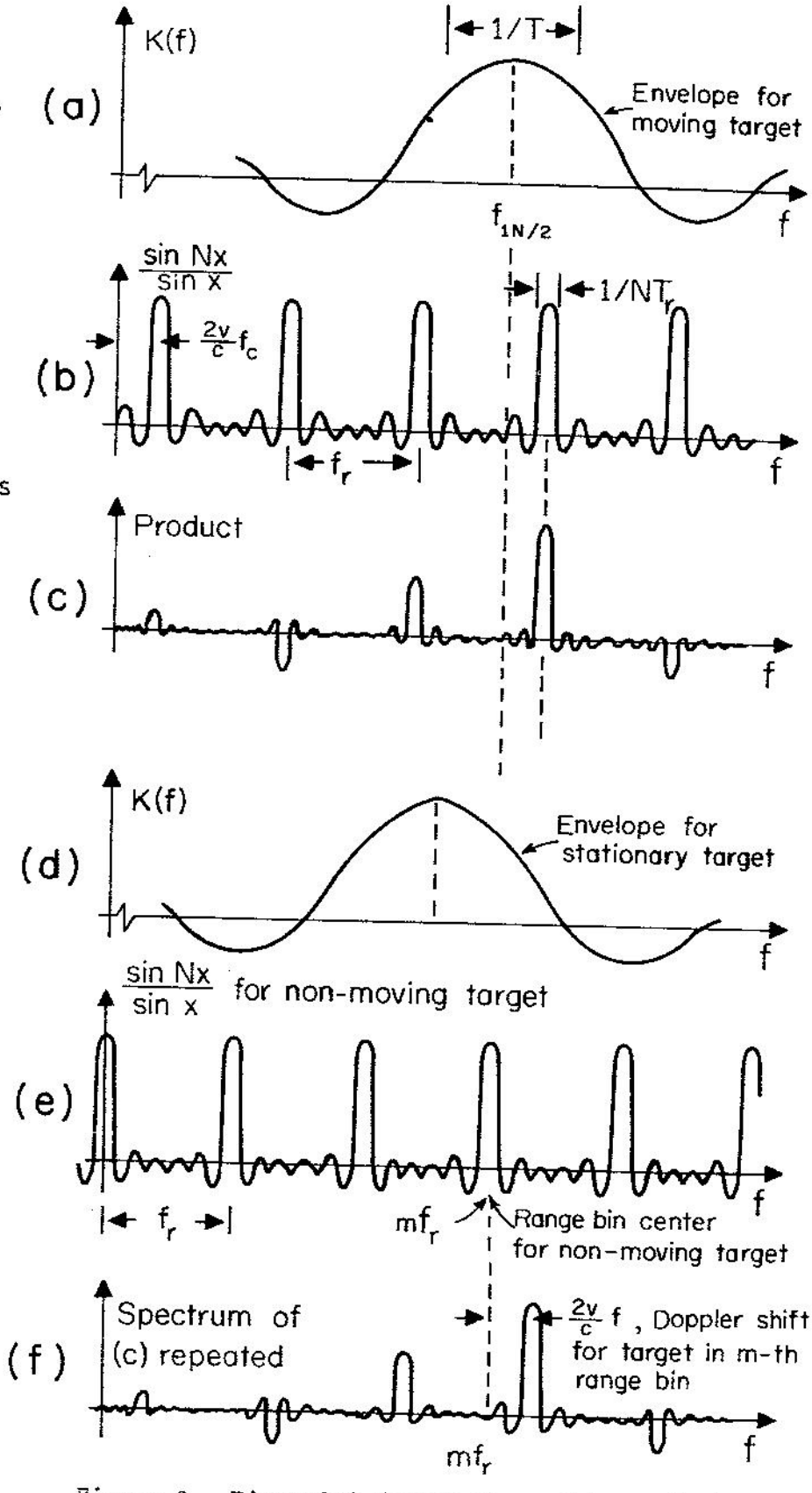

Figure 6. Pictorial description of long single FFT processing over N pulses.

of the broader function, corresponding to $f_r = 1/T_r$ Hz (i.e., a 1.5 km bin here), while the Doppler resolution is essentially the width of the narrower line, corresponding to $1/NT_r$ Hz, the coherent integration time.

The frequency axis after the long FFT can thus be broken up into M/2 coarse range bins of width $1/T_r$ Hz; within each range bin, finer frequency divisions then correspond to the Doppler spectrum of the target. In particular, there are N Doppler bins per range bin, corresponding to a Doppler resolution of $1/NT_r$ Hz. It seems proper therefore to center each range bin on a zero-Doppler line. The centers of each range bin--as shown in figure 6--are thus located at mf_r(multiples of the PRF) along the frequency axis, and extend $\pm f_r/2$ away from this central, zero-Doppler position. Thus we can take the plot along the positive frequency axis and divide it into M/2 pieces, each centered at mf_r where $0 < m < M/2$. Each piece then represents the Doppler spectrum of an individual range bin. Or, we can have the computer do the "dividing" for us, displaying each range bin however we choose. For example, range bins could be lined up behind each other, closely spaced, to give a 3-dimensional range-Doppler-intensity display. Note also that each range bin--and the resulting Doppler spectrum thus obtained--is similar to the Fourier transform over a given column in the preceding section; both are range bins containing a Doppler spectrum with the same resolution and width. THEREFORE THE TWO PROCESSING TECHNIQUES YIELD IDENTICAL RESULTS.

A little thought will also show that this technique will work for distributed targets. For example, if we have many targets over several range bins but at the same velocity, we will effectively have several K(f) functions in (23), but centered on slightly different positions. The $\sin N\alpha/\sin\alpha$ functions for the Doppler will be identical. Thus in effect the target at a given Doppler will appear in several range bins, as it should, but at the same discrete velocity in each.

8. NUMBER OF COMPUTER OPERATIONS REQUIRED

The possibility exists with present day computers--especially "minicomputers" of the NOVA and HP 2110/2115 variety--that the range-Doppler processing described above can be done in real time. Such processing for HF radars has in fact been done digitally in real time by

several groups for both discrete targets and sea scatter, using no more than a single HP 2115 minicomputer. To ascertain whether such is possible for a given application, we must know the number and size of the digital words to be stored and processed per second.

The FFT process is known to require $L\log_2 L$ operations for a linear array of L numbers. Let us first analyze the total number of operations required by the double FFT. We first do an FFT on a pulse, using M samples; this requires $M\log_2 M$ operations. Next we begin transforming over each of the M/2 columns; each now contains a real and imaginary word for a total of M words. With N elements in a column, $N\log_2 N$ operations are required for the FFT on each column. For M column words, this gives $MN\log_2 N$ operations. Thus the sum of operations required in the first and second sets of FFT processing is

$$MN\log_2 M + MN\log_2 N = MN(\log_2 M + \log_2 N) = MN\log_2 MN \qquad (25)$$

operations.

The number of operations required in the single long FFT is simple to calculate. With N pulses and M samples per pulse, we have MN total samples per transform. This therefore requires $MN\log_2 MN$ operations. THIS IS IDENTICALLY THE SAME NUMBER AS FOR THE DOUBLE FFT!

Normally the FFT requires that the number of samples to be transformed be an integer power of 2. For the double FFT process therefore, both M and N must be powers of 2 (e.g., 256 and 128, 32 and 64, etc.; just so M and N individually are greater than the number required by the sampling rate and Doppler resolution). For the single, long FFT, the product MN must be a power of two, and hence again M and N must individually be powers of two.

In both cases, MN elements must be accumulated and stored for processing; this dictates the size of the required core and/or disc storage. The entire number of $MN\log MN$ operations must be performed every NT_r seconds if the process is to be done in real time. This requires that $(M\log_2 MN)/T_r$ computer operations per second be done (not including time for buffering and display functions). Thus the obvious way to reduce the required data rate--if such is necessary--is to lower M, the number of range bins. Since M is equal to $2f_{1max}T_r$, we must

reduce f_{1max}, the maximum IF frequency per pulse. This does not necessarily require one to reduce the range resolution. For example, suppose for our example that instead of observing all ranges from 0 to 150 km with a 1.5 km resolution (giving M=200), we decided that we only wanted to observe the window between 126 km and 150 km, but still with 1.5 km resolution. This gives conceptually M=32 or M/2=16 range bins. To achieve this, one merely slides the linear sweep delay in the receiver so that instead of varying between 84 and f_{1max}=100 Hz, f_1 now runs between 0 and f_{1max}=16 Hz. Then the M=32 samples are adequate for the T_r=1 second pulse repetition interval.

Finally, the number of bits required per word also affects the data rate to some extent. The processor dynamic range depends upon the bits per word because of quantization error. Thus the dynamic range is optimally 6b decibels, where b is the number of (binary) bits per word. Currently about 80 dB dynamic range can be realized by digital processors without too much difficulty, requiring 14 bit words and a 14-bit A/D convertor.

9. WINDOWING AND WEIGHTING

In all of the preceding sections, we assumed a square pulse at frequency f_1, and N such pulses all with the same amplitude. As a result we arrived at $\sin x/x$ and $\sin Nx/\sin x$ functions in the frequency domain for the target echoes. Both functions have rather high, objectionable sidelobes: the first sidelobe of the $\sin x/x$ function is only 13 dB down from the main lobe, while the average sidelobe level of the $\sin Nx/\sin x$ function between main lobes is only down 20 dB. Thus some of the sidelobes from a single target--as illustrated in figure 6--are quite high and could be mistaken for other targets.

The remedy for this is the same as that taken by antenna designers to reduce sidelobes: use an amplitude taper across the original function before Fourier transforming. This technique is currently being used in nearly all radar digital processing schemes. The common amplitude taper--or weighting--used across the time window is the Taylor weight (although Hamming and cosine-squared weights (Blackman,1958; Nathanson, 1969) are sometimes used). This results in average sidelobes down 40-50 dB

below the main lobe. The only bad effects of such weighting are the slight broadening of the main lobe (by as much as 40% in some cases at the 3-dB point) and a drop of 1-2 dB in signal-to-noise ratio due to attenuation of the original received signal at the edges of the window.

For both types of processing described above, two weighting functions are normally performed digitally. The first is to weight the M samples within the pulse according to the selected function (e.g., Taylor weighting). The next is to weight the N pulses to be used in the coherent integration by the selected technique. Both weighting processes across the two respective windows of T_r and NT_r seconds are normally required to keep both the range and Doppler sidelobes unobjectionable.

10. RULES FOR SIGNAL DESIGN

Here we give a simple, stepwise procedure for calculating the signal parameters required for a given set of backscatter radar or sounder specifications. We assume that the following parameters describing the system are given: (i) f_c, the carrier frequency, in Hertz; (ii) R_w, the range window width to be calculated and displayed, in meters; (iii) v_M, the maximum target velocity in m/s; (iv) ΔR, the range resolution desired, in meters; (v) Δv, the velocity resolution desired, in m/s.

With these parameters given, the following four steps are to be used to calculate the following four FM/CW signal and processing parameters: (i) B, the signal bandwidth, or frequency excursion, in Hertz; (ii) T_r, the pulse repetition interval, in seconds; (iii) N, the number of pulses of period T_r needed for a single coherent processing operation; and (iv) M, the number of samples needed per pulse interval, T_r.

(1) $B = c/(2\Delta R)$, where c is the wave propagation velocity in the medium.

(2) $T_r = 1/f_r$, where $f_r = 2f_{DM}$, f_{DM} being the maximum target Doppler shift, given by $f_{DM} = (2v_M/c)f_c$.

(3) $N = T_c/T_r$, where T_c, the total coherent integration time is the reciprocal of the desired Doppler resolution, Δf_D, where $\Delta f_D = (2\Delta v/c)f_c$.

(4) $M = 2R_W/\Delta R$ samples per pulse interval, T_r.

In the above, we have assumed that f_c, R_W, v_M, ΔR, and Δv were all given and that B, T_r, N, and M were to be found. In practice, the size of the computer and data handling rate will often limit M and N. Thus one usually iterates until an acceptable compromise is achieved, i.e., he varies his requirements for R_W, ΔR, and Δv until values of M and N are obtained within the capacity of his machine.

11. SATISFACTION OF REQUIRED ASSUMPTIONS

In the course of the analysis herein, certain assumptions were made, upon which the desired output is dependent. If these are *not* satisfied, quadratic and other types of distortions will result which reduce or limit the achievable signal-to-noise ratio. Having derived B, T_r, M, and N from the rules of the preceding sections, one can quickly check the following criteria to see whether the optimum processing gain will be realized.

(1) $\frac{1}{2} BT_r(2v_M/c)^2N^2 \ll 1,$

$B(2v_M/c)(2R_W/c)N \ll 1,$

$B(2v_M/c)T_r/4 \ll 1$.

Satisfaction of the above conditions was assumed in going from (12) to (13) for the phase; if one or more of these conditions are not satisfied, distortion will reduce the achievable processing gain.

(2) $v_M NT_r < \Delta R.$

This merely means that the target is not traveling so fast that it moves through several range bins within one coherent integration period, NT_r. If the inequality fails, it simply means that the echo will appear in several range bins, but with a proportionately reduced amplitude in each.

(3) $dv/dt \;\; NT_r < \Delta v.$

This assumption--heretofore unmentioned--concerns the rate of change of radial target velocity (or radial acceleration). It has been assumed throughout the analysis that the targets under consideration have a constant, nonaccelerating velocity. Small radial accelerations can be tolerated, but if dv/dt is sufficiently large that the above inequality fails, then the echo will appear spread into several Doppler bins with proportionately reduced amplitude in each.

12. SUMMARY

Despite statements often seen concerning "chirp" (i.e., linearly swept frequency) signals used with microwave radars, *there is no ambiguity* between target range and velocity for processing done in the straightforward digital manner described in this note.* Furthermore, two seemingly different digital processing schemes are described and analyzed herein, which will produce exactly the same pulse-Doppler (range-velocity) output. Both employ the FFT; the first uses a shorter FFT many times, while the second uses only one long FFT to produce the same coherent pulse-Doppler map. Both techniques work equally well for discrete targets (such as an aircraft), as well as for continuous or distributed target complexes (such as ocean waves, rain, atmospheric turbulence, etc.), and display the targets in their appropriate range-velocity perspective.

Identically the same total number of FFT operations is required for both techniques; the same data rate (A/D convertor rate) is required in each case also, i.e., $(2R_W/\Delta R)\times 2\times(2v_M/c)f_c$ words per second. Here, R_W is the range window length to be examined, ΔR is the range resolution desired, v_M is the maximum target velocity to be encountered, c is the free space wave propagation velocity, and f_c is the carrier frequency. The choice of whether to use the multiple vs the single FFT processing technique then rests with the availability of appropriate equipment. For

*Perhaps the ambiguity occurring in the microwave systems is attributable to the analog pulse compression techniques commonly employed there, such as the dispersive delay line. Here the technique used is more properly described as a coherent correlator followed by pulse-Doppler processing, rather than time-domain pulse compression. The difference between the two techniques results in the elimination of the ambiguity for type of processing described here.

example, small computers may be limited in the size of a single FFT they can handle; in this case, the multiple FFT technique having smaller unit size may be required. On the other hand, special hard-wired FFT computers are currently available (called "FFT boxes"). These can perform a fairly large, fixed-length transform very rapidly because of their specialized construction, and are used as one component in the overall digital processing system. Here, the single long FFT is usually more efficient because the need for continual, interactive storage/retrieval of elements in matrix/fashion demanded by the multiple FFT scheme is eliminated.

13. REFERENCES

Blackman, R. B. and J. W. Tukey (1958), *The Measurement of Power Spectra*. (Dover Publications: New York, pp. 14-15).

Eddy, F. N. (1973), Analysis of repeated chirp system (in preparation), The MITRE Corporation, Bedford, Mass. (prepared for Rome Air Development Center).

Nathanson, F. E. (1969), *Radar Design Principles*. (McGraw-Hill: New York, pp. 520-530).

Sweeney, L. E., Jr., W. B. Zavoli, and D. E. Westover (1971), Processing of swept-frequency-CW HF backscatter signals using the two-dimensional FFT, Technical Report No. 6, Ionospheric Dynamics Laboratory, Stanford Research Institute, Menlo Park, Calif., Contract No. N00014-70-C-0413.

☆GPO 1973 — 784-572/1234 REGION NO. 8